REFERENCES AND NOTES

1. For review, J. N. George, A. T. Nurden, D. R. Phillips, *N. Engl. J. Med.* **311**, 1084 (1984); L. A. Fitzgerald and D. R. Phillips, in *Platlet Immunobiology*, T. J. Kunicki and J. N. George, Eds. (Lippincott, Philadelphia, 1989), pp. 9–30.
2. P. J. Newman, in *Platelet Immunobiology*, T. J. Kuniki and J. N. George, Eds. (Lippincott, Philadelphia, 1989), pp. 148–165.
3. P. J. Newman *et al.*, *J. Cell. Biol.* **103**, 81 (1986); L. A. Fitzgerald *et al.*, *J. Biol. Chem.* **260**, 10893 (1985); E. F. Plow *et al.*, *Proc. Natl. Acad. Sci. U.S.A.* **83**, 6002 (1986); J. C. Giltay *et al.*, *Blood* **73**, 1235 (1989).
4. R. O. Hynes, *Cell* **48**, 549 (1987).
5. P. J. Newman *et al.*, *Throm. Res.* **27**, 221 (1983).
6. R. Hall *et al.*, *Nature* **311**, 379 (1984); C. Weinberger *et al.*, *Science* **228**, 740 (1985). In this procedure, β-galactosidase fusion proteins from individual plaque-purified antibody-positive clones are immobilized on nitrocellulose membranes and are used to "select" from the polyspecific screening antiserum those antibodies capable of binding the specific epitopes encoded by each individual fusion protein. The specific antibodies are eluted from the washed membranes and specificity is determined by immunoblot analysis of whole platelet or endothelial cell SDS lysates. Binding to a distinct 130-kD component was visualized with an alkaline phosphatase-conjugated second antibody followed by a 5-bromo-4-chloro-3-indolyl phosphate/nitro blue tetrazolium salt substrate pair.
7. S. M. Goyert *et al.*, *J. Immunol* **137**, 3909 (1986).
8. Fourth International Workshop on Human Leukocyte Differentiation Antigens, Vienna, Austria. Detailed proceedings to be published by Oxford University Press in January 1990. Reviewed in W. Knapp *et al.*, *Immunology Today* **10**, 253 (1989). Other workshop antibodies belonging to the CD31 cluster include TM3 [H. Ohto *et al.*, *Blood* **66**, 873 (1985)] and HEC-75 [J. A. van Mourik, O. C. Leeksman, J. H. Reinders, P. G. de Groot, J. Zandbergen-Spaargaren, *J. Biol. Chem.* **260**, 11300 (1985)]. TM3 binds to myeloid and monocytoid, but not erythroid, hematopoietic cells, and can inhibit endotoxin-induced chemotactic migration of neutrophils and monocytes through a micropore filter of a Boyden chamber. HEC-75 is a shared component of platelets and endothelium, and displays a membranous staining pattern in cultured endothelial cells at confluent or near-confluent densities.
9. W. A. Muller, C. M. Ratti, S. L. McDonnell, Z. A. Cohn, *J. Exp. Med.* **170**, 399 (1989). PECAM-1 was visualized on fixed, permeabilized, cultured human umbilical vein endothelial cells using the MAb hec7 and the peroxidase–anti-peroxide technique.
10. P. J. Newman *et al.*, unpublished observations.
11. PECAM-1 was isolated from human platelets by immunoaffinity chromatography using the MAb WM59. WM59 (IgG_1 subclass) was produced by immunizing mice with washed human platelets. Platelet lysates precleared with WM59 antibody are devoid of material reactive with anti–PECAM-1 fusion protein antisera.
12. The complete nucleotide sequence for PECAM-1 is available in the EMBL, GenBank, and DDBJ Nucleotide Sequence Databases under the accession number M28526.
13. J. Kyte and R. F. Doolitte, *J. Mol. Biol.* **157**, 105 (1982).
14. G. von Heijne, *Nucleic Acids Res.* **14**, 4683 (1986).
15. Glutamine readily cyclizes to pyroglutamate, which is not cleavable during Edman degradation.
16. The nine predicted Asn-linked amino acids are located at residues 25, 57, 124, 274, 293, 317, 329, 426, and 524 of the mature polypeptide chain.
17. Tyr^{686} of PECAM-1 is located in a favorable environment for phosphorylation, as tyrosine kinase substrates often are positioned seven residues to the COOH-terminal side of a Lys or an Arg, and three or four residues COOH-terminal to an Asp or Glu. T. Patschinsky *et al.*, *Proc. Natl. Acad. Sci. U.S.A.* **79**, 973 (1982); T. Hunter, *J. Biol. Chem.* **257**, 4843 (1982); J. A. Cooper, F. S. Esch, S. S. Taylor, T. Hunter, *ibid.* **259**, 7835 (1984).
18. T. Hunkapiller and L. Hood, *Nature* **323**, 15 (1986); A. F. Williams, *Immunology Today* **8**, 298 (1987); ——— and A. N. Barclay, *Annu. Rev. Immunol.* **6**, 381 (1988).
19. S. Benchimol *et al.*, *Cell* **57**, 327 (1989).
20. D. E. Staunton *et al.*, *ibid.* **52**, 925 (1988).
21. B. A. Cunningham *et al.*, *Science* **236**, 799 (1987); M. Moos *et al.*, *Nature* **334**, 701 (1988); A. L. Harrelson and C. S. Goodman, *Science* **242**, 700 (1988); M. A. Seeger, L. Haffley, T. C. Kaufman, *Cell* **55**, 589 (1988); B. Ranscht, *J. Cell. Biol.* **107**, 1561 (1988).
22. A. B. Edmundson, K. R. Ely, E. E. Abola, M. Schiffer, M. Panagiotopoulos, *Biochemistry* **14**, 3953 (1975).
23. J. Novotny and C. Auffray, *Nucleic Acids Res.* **12**, 243 (1984); P. Y. Chou and G. D. Fassman, *Biochemistry* **13**, 211 (1974).
24. D. J. Lipman and W. R. Pearson, *Science* **227**, 1435 (1985).
25. C. J. Sherr *et al.*, *Cell* **41**, 655 (1985); L. Coussens *et al.*, *Nature* **320**, 277 (1986).
26. L. T. Williams, *Science* **243**, 1564 (1989); M. T. Keating *et al.*, *J. Biol. Chem.* **263**, 12805 (1988).
27. J. W. White and D. R. Littman, *Cell* **56**, 725 (1989).
28. S. Oikawa, H. Nakazato, G. Kosaki, *Biochem. Biophys. Res. Commun.* **142**, 511 (1987).
29. R. G. K. Gronwald *et al.*, *Proc. Natl. Acad. Sci. U.S.A.* **85**, 3435 (1988).
30. Y. Yarden *et al.*, *Nature* **323**, 226 (1986).

31. We thank C.-J. Edgell and D. Ginsberg for providing endothelial cell cDNA libraries and S. Goyert for providing the anti-CD31 International Workshop antibody, SG134. W.A.M. is the recipient of a Pew Scholarship and an RJR-Nabisco Research Scholars Award. Supported by grant HL-40926 (to P.J.N.) from the National Institutes of Health.

2 October 1989; accepted 8 January 1990

Ribozymes as Potential Anti–HIV-1 Therapeutic Agents

NAVA SARVER,* EDOUARD M. CANTIN, PAIROJ S. CHANG, JOHN A. ZAIA, PAULA A. LADNE, DELILAH A. STEPHENS, JOHN J. ROSSI

Certain RNA molecules, called ribozymes, possess enzymatic, self-cleaving activity. The cleavage reaction is catalytic and no energy source is required. Ribozymes of the "hammerhead" motif were identified in plant RNA pathogens. These ribozymes possess unique secondary (and possibly tertiary) structures critical for their cleavage ability. The present study shows precise cleavage of human immunodeficiency virus type 1 (HIV-1) sequences in a cell-free system by hammerhead ribozymes. In addition to the cell-free studies, human cells stably expressing a hammerhead ribozyme targeted to HIV-1 *gag* transcripts have been constructed. When these cells were challenged with HIV-1, a substantial reduction in the level of HIV-1 *gag* RNA relative to that in nonribozyme-expressing cells, was observed. The reduction in *gag* RNA was reflected in a reduction in antigen p24 levels. These results suggest the feasibility of developing ribozymes as therapeutic agents against human pathogens such as HIV-1.

INVESTIGATORS HAVE SHOWN THE ability of antisense RNAs to impair gene expression (*1*) and have suggested the use of these molecules as antiviral and anticancer agents. However, there are several limitations to this approach imposed, in part, by the stoichiometric nature of the inhibition. Alternatively, the observation that certain RNA molecules (ribozymes) possess enzymatic, self-cleaving activity (*2–5*) suggests that antisense molecules could be developed that not only form RNA-RNA hybrids, but also catalytically cleave a phosphodiester bond in the target RNA strand. Because the catalytic RNA would not be consumed during the cleavage reaction, a large number of substrate molecules could be processed (Fig. 1). Two structural motifs, hammerhead (*5, 6*) and hairpin (*7*), have thus far been described as intermediates in these self-cleavage reactions.

Ribozymes in the hammerhead family share a high degree of similarity in primary and secondary structure (*6, 8, 9*). The hammerhead consists of three stems and a catalytic center containing 13 conserved nucleotides (5′GAAAC$(N)_n$GUN$(N)_n$CUGA(N)GA3′) (Fig. 2). Natural catalytic centers may be formed by contiguous regions in the RNA (*6, 8*) or by regions separated by a large number of nucleotides (*5, 10*). Cleavage occurs 3′ to the GUX triplet where X can be C, U, or A (*11–13*), generating 2′,3′-cyclic phosphate and 5′ hydroxyl termini (*4, 5*). The essential constituents for the hammerhead can be on separate molecules, with one strand serving as a catalyst and the other as a substrate (*11, 12*) (Fig. 1). Further,

N. Sarver, Developmental Therapeutics Branch, Division of Research and Development Program, Division of AIDS, National Institute of Allergy and Infectious Diseases, Bethesda, MD 20892.
E. M. Cantin, J. A. Zaia, P. A. Ladne, D. A. Stephens, City of Hope Medical Center, Duarte, CA 91010.
P. S. Chang, Department of Molecular Genetics, Beckman Research Institute of the City of Hope, Duarte, CA 91010 and Department of Biochemistry, Loma Linda University, School of Medicine, Loma Linda, CA 92350.
J. J. Rossi, Department of Molecular Genetics, Beckman Research Institute of the City of Hope, Duarte, CA 91010.

*To whom correspondence should be addressed.

RNA sequences containing only the conserved cleavage domain (GUX) can serve as compatible substrates (*13, 14*).

To show the use of ribozyme-based reactions as a potential therapy for human immunodeficiency virus type 1 (HIV-1) infection, we have designed hammerhead motifs that are stably expressed and are capable of cleaving HIV-1 RNA in a complex cellular environment. Ribozymes targeted to HIV-1 *gag* caused a reduction in HIV *gag* RNA with a concomitant decrease in the *gag*-encoded protein, HIV-1 p24 antigen.

Two distinct hammerhead designs were used. Substrate A (Fig. 2a) contained two of the four conserved domains making up the catalytic center. These sequences, 5′GAAAC3′ and 5′GUX3′ (the latter being the cleavage domain), represent two HIV-1 *gag* RNA regions only 7 nucleotides (nt) apart from each other. Substrate B (Fig. 2a) contained only the 5′GUX3′ cleavage site. In each case, the respective catalyst supplied the remaining consensus domains as well as the complementary sequences required to complete a stable hammerhead configuration. Design A and B catalyst RNAs were transcribed with the T7 RNA polymerase system. HIV-1 RNA substrates were similarly generated from cloned DNA fragments harboring the appropriate HIVHXB2 (*15*) segments. All RNAs were separated by electrophoresis and purified in acrylamide-urea gels.

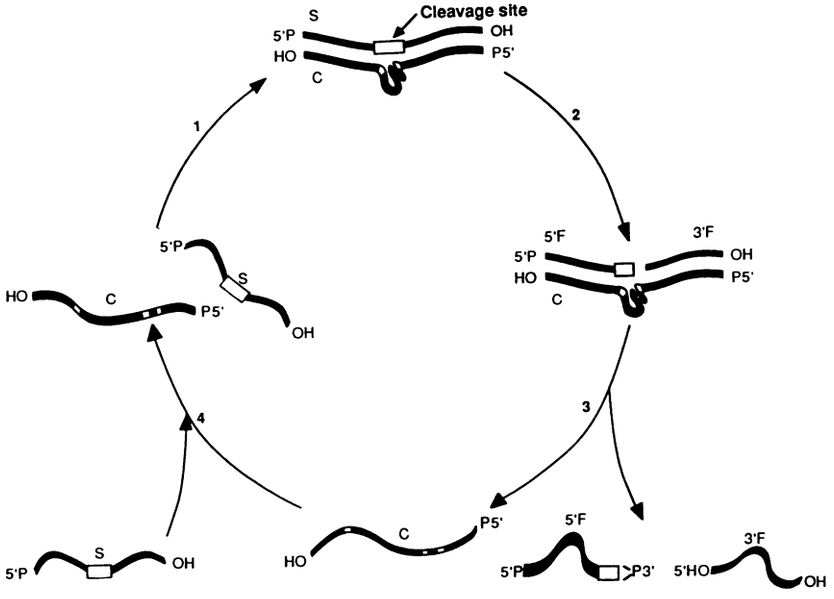

Fig. 1. Catalytic cycle of ribozyme-mediated cleavage (*3–6*). Starting at the 9 o'clock position in the cycle, the catalyst (C) and substrate (*S*) RNAs associate by virtue of complementary sequences surrounding the catalytic center to form a complex, thereby forming the secondary configuration required for cleavage. In the presence of cations, cleavage of substrate occurs, generating the two cleavage products (5′F and 3′F). Next, the complex dissociates, releasing 5′F and 3′F, and the catalyst is again available to combine with the next substrate strand. The unique feature of the reactions is the 2′,3′-cyclic phosphate and 5′ hydroxyl termini at the cleavage site.

The reaction products generated by this strategy are shown in Fig. 2b. Both catalytic designs induced cleavage of substrate RNA, although catalyst B did so much more efficiently. In fact, almost all of substrate B was consumed when 1 pmol each of substrate and catalyst were used with a 14-hour incubation period at 37°C. In contrast, 25 to 30% of substrate A remained intact under the same experimental conditions. Concomitant with the reduction in substrate, each cleavage reaction generated two new products corresponding to the 5′ and 3′ portions of the substrate (Fig. 2b, 5′F and 3′F). The length of each fragment agreed with the predicted size.

To confirm the specificity of the cleavage reaction, we performed dideoxyribonucleotide sequencing with a synthetic deoxyribonucleotide primer complementary to *gag* sequences downstream of the expected cleavage site. This analysis confirmed that cleavage occurred precisely as predicted, immediately 3′ to GUX. It also showed, albeit indirectly, that the heterogeneity observed with the smaller cleavage product (Fig. 2b, 3′F) was caused by premature termination stops during the in vitro transcription reaction rather than imprecise cleavage events at multiple sites (*16*).

One potential way to stabilize the catalyst in an intracellular environment is through the addition of a 5′ GpppG cap structure. To ascertain that such modification does not impede the cleavage process, we used unmodified and capped catalysts. Uncapped and capped catalysts were very similar in

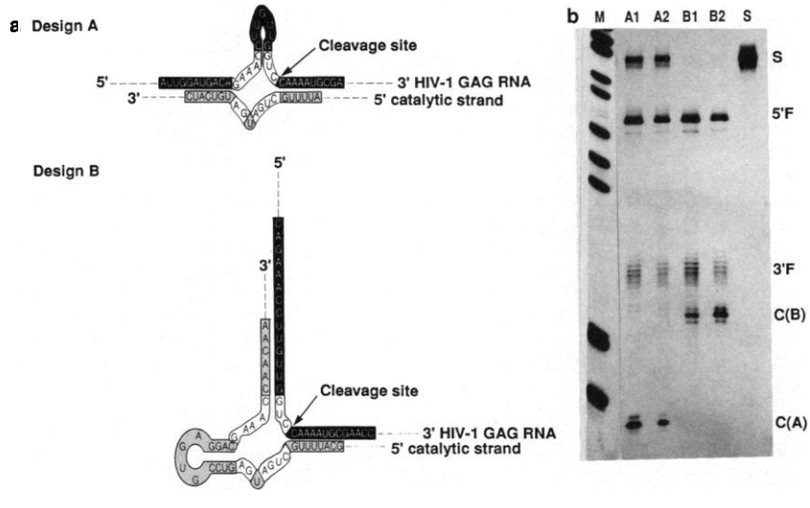

Fig. 2. Comparison of the activities of two hammerhead catalytic RNA designs targeted to the same cleavage site. (**a**) Base-pairing of the catalytic strands with the HIV-1 *gag* RNA template for design A and design B is depicted on the left. Cleavage reactions using designs A and B are presented on the right. Reaction conditions were as follows: Catalytic and substrate RNAs were labeled with [α-^{32}P]uridine triphosphate. The catalytic and substrate RNAs (1 pmol of each) were mixed in a 10-μl reaction volume containing 50 m*M* tris-HCl, *p*H 7.5, and 1 m*M* EDTA. The mixture was heated to 95°C for 2 min, quick-cooled on ice, 10 m*M* $MgCl_2$ was added, and then it was incubated at 37°C for 14 hours. (**b**) The resulting products were analyzed in an 8% polyacrylamide–7*M* urea gel in tris-borate EDTA (TBE) buffer and autoradiographed. Substrate RNA is 138 nt long, encompassing nucleotides 1711 to 1789 in HIVHXB2 (*15*) (GenBank accession number K03455) plus an additional 60 nt from the polylinker; the sequences for the catalytic RNAs are shown. Lane M, Hpa II–digested pBR322 molecular weight markers; lane A1, unmodified catalytic RNA A plus substrate; lane A2, 5′ GpppG-capped catalytic RNA A plus substrate; lane B1, unmodified catalytic RNA B plus substrate; lane B2, 5′ GpppG-capped unmodified catalytic RNA B plus substrate; and lane S, substrate alone incubated under the same reaction conditions. A and B refer to the respective designs in (a). S, substrate RNA; C, catalytic RNA; 5′F, 5′ cleavage product; and 3′F, 3′ cleavage product.

processing an identical substrate under these experimental conditions (Fig. 2b, compare A1 to A2 and B1 to B2).

These results show that relative to catalyst A, catalyst B is more efficient in completely cleaving its substrate. This may be because of a more rapid formation of an active hammerhead configuration, since three of the four conserved domains reside along a single strand. Because the substrate B design contains only the cleavage domain, a greater number of RNA sequences can be used as targets. Substrate B was, therefore, the prototype used in subsequent experiments.

Implementation of ribozymes for therapeutic use will depend on the ability of RNA catalysts to function in a complex cellular milieu. Specifically, it is necessary to determine whether (i) stable expression of the catalyst can be achieved; (ii) nonspecific cellular or viral RNAs present in infected cells would impede the association of the catalyst with target RNA, and thereby inhibit cleavage; (iii) long mRNA targets are accessible for cleavage; (iv) vector-derived, noncomplementary flanking sequences in the catalyst interfere with specific cleavage; and (v) endogenous ribozyme expression is toxic to cells. To study these questions, we cloned an anti-*gag* catalyst gene in a mammalian expression vector (*17*) (Fig. 3), which uses the constitutive human β-actin promoter to drive transcription. The resulting vector was transfected into CD4$^+$ HeLa cells (*18*), and stable guanosyl-phosphoribosyltransferase (GPT)–expressing colonies were isolated. Several individual clones, as well as pooled populations, were examined for expression of the catalyst with an RNA-based polymerase chain reaction assay (PCR) (*19*) (Fig. 3). In each case tested, catalytic RNA was detected. The presence of anti-*gag* ribozyme was confirmed by Northern (RNA) gel analysis of polyadenylated [poly(A)$^+$] RNA from expressing cells: a broad band of approximately 450 nt, 200 to 250 nt longer than the expected primary transcript, was detected (*16*). The additional length of the hybridizing fragment is attributable to a poly(A)$^+$ tail.

Next, we studied the ability of these molecules to cleave viral RNA in acute infections. Cell lines expressing the catalytic RNA, as well as untransformed parental cells, were challenged with HIV-1 as described (*20*). PCR analysis was done on total RNA isolated 7 days after infection (Fig. 4a): GAG1 is a first-strand primer of opposite polarity to HIV-1 RNA, and it is located within the *gag* region 220 nt downstream of the expected cut site. GAG2 and LTR1 are second-strand primers of the same polarity as the viral RNA. GAG2 is 15 nt downstream of the cut site and LTR1 is 240 nt upstream. In the absence of cleavage, two species are expected: an intact 480-nt fragment extending

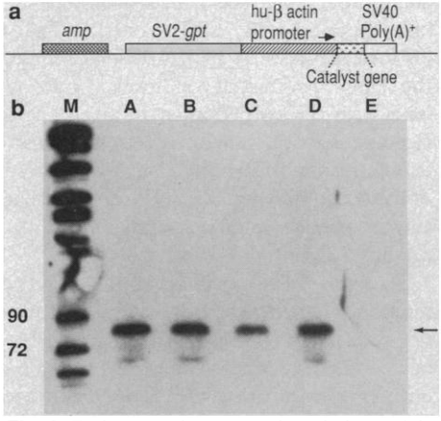

Fig. 3. Endogenously expressed catalytic RNA in HeLa CD4$^+$ cells. (**a**) A schematic diagram of the mammalian expression vector containing an anti-*gag* hammerhead catalyst gene is shown. This vector, derived from p-hu β APr-1-gpt (*17*) was introduced into HeLa CD4$^+$ cells (*18*) by lifofection (materials and protocol from BRL) and transformants were selected based on stable expression of Gpt. Total RNAs isolated from positive transformants were used as templates for RNA-based PCR analyses. Primer 1 was complementary to the SV40 sequences, downstream of the catalyst gene and upstream of the poly(A)$^+$ addition site; primer 2 was of the same polarity as the first 17 nt of the catalyst gene. The probe used to detect the amplified products was complementary to catalyst sequences downstream of primer 2. The PCR reactions were carried out by first mixing 200 ng of total RNA from the various transformants with 20 pmol of primer 1 in 1× GeneAmp buffer (Taq polymerase buffer; Perkin-Elmer–Cetus), 200 μmol of each deoxynucleoside triphosphate (dNTP) and 2 units of avian myeloblastosis virus (AMV) reverse transcriptase (Life Sciences) in a total volume of 48 μl and incubating at 40°C for 3 min. Reaction mixtures were overlaid with 50 μl of mineral oil and placed in a DNA Thermal Cycler for 40 cycles at 94°C for 1 min, 47°C for 1.5 min, and 72°C for 1.5 min, with 5 s added at each cycle. The PCR-amplified products were separated by electrophoresis in a 6% polyacrylamide–7*M* urea gel in TBE buffer, and electroblotted to a nylon membrane (Zeta-Probe, Bio-Rad). Hybridization of a labeled ribozyme-specific oligonucleotide probe was carried out as described previously (*23*). (**b**) The expected size of the PCR-amplified product is 80 nt (arrow). The lanes depict DNAs amplified from catalytic RNA templates obtained from the various p-hu β APr-1-gpt-gagribo transformed clones. Lane M, Hpa II–digested pBR322 molecular weight marker (90- and 72-kb sizes are shown to the left); lanes A, C, and D, isolated transformed clones; lane B, pooled transformants; and lane E, untransformed HeLa CD4$^+$ parental cells.

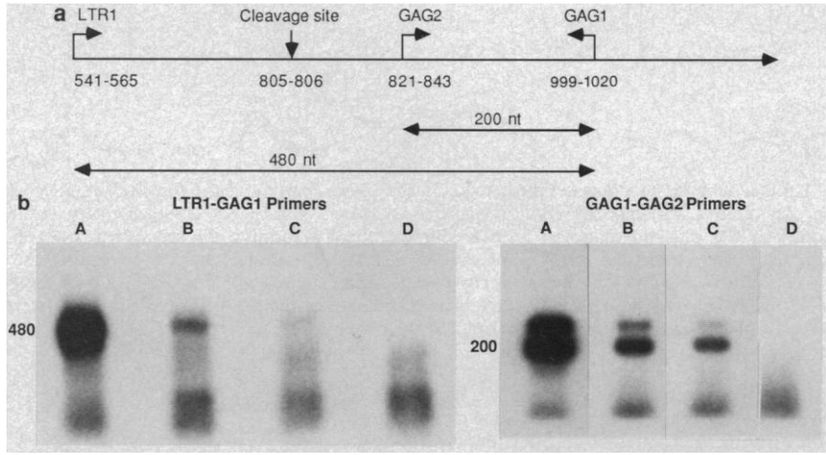

Fig. 4. Ribozyme-mediated cleavage of *gag* RNA after challenge with HIV-1. Monolayers of HeLa CD$^+$ cells in 24-well culture plates were washed twice with Dulbecco's modified Eagle's medium (DMEM) and then treated with 200 μl of DMEM containing 10% fetal bovine serum (FBS) and Polybrene (10 μg/ml). A 20-μl inoculum of HIV-1 was added to each well (*20*). Adsorption was at 37°C for 2 hours. The cells were then washed twice with DMEM and fed with 1 ml of DMEM containing 10% fetal calf serum. Cells were incubated for 7 days and then assayed for viral RNA and soluble p24 with a commercially available kit (Du Pont). (**a**) Relative position of the cleavage site within the *gag*. Primers are described in the text. The conditions for the PCR were as described in Fig. 3 with the following exceptions: Reverse transcription was performed for 3 min at 37°C with only primer GAG1 and 2 units of AMV reverse transcriptase in GeneAmp Taq polymerase buffer. After this reaction, the second primer and 2.5 units of Taq polymerase were added. For LTR1 and GAG1, the cycling conditions were as follows: 94°C for 2 min, 50°C for 1 min, and 72°C for 1.5 min for 50 cycles. For GAG2 and GAG1, the conditions were 94°C for 2 min, 47°C for 3 min, and 72°C for 40 s with an additional 3 s every cycle for the first 25 cycles. The products of the PCR reactions were treated as described previously (*23*) including electrophoresis in 1.5% agarose in TBE buffer, alkaline blotting to a nylon membrane, and hybridization with a ^{32}P-labeled oligonucleotide probe complementary to sequences in between GAG1 and GAG2. (**b**) PCR amplification of HIV-1 RNA. Each lane contained DNA amplified from 0.5 μg of total RNA from HIV-1–infected cells. The sizes for the PCR products are shown. Lanes A, untransformed HeLa CD4$^+$ parental cells; lanes B, cloned cell line transformed with anti-*gag* catalytic RNA; lanes C, pooled clones transformed with the anti-*gag* catalytic RNA; and lanes D, PCR contamination control lacking template. Infection of the cells with HIV-1 was as previously described (*20*).

from GAG1 to LTR1, which encompasses the cleavage site, and a smaller, 200-nt fragment delineated by GAG1 and GAG2. If cleavage of *gag* RNA has occurred, a reduction in the level of the 480-nt species relative to the 200-nt fragment is expected. Untransformed cells (Fig. 4b, lanes A) contained similar levels of the 480- and 200-nt fragments, as expected. In contrast, cloned cells expressing the catalytic RNA contained significantly less of the larger, 480-nt fragment relative to the smaller, 200-nt species (lanes B). This was more striking with an RNA sample extracted from pooled clones, where the 480-nt fragment was almost undetectable (lanes C). Since the 200-nt fragment is derived from sequences not subject to cleavage, the relative reduction of this fragment in ribozyme-containing cells versus parental cells shows that the ribozyme is cleaving incoming viral RNA.

Quantitative determination of soluble p24 antigen at 7 days after infection showed a marked diminution in the amount secreted from transformed compared to parental cells. For the samples shown in Fig. 4b, the p24 concentrations were 0.14 ng/ml for cloned transformants and 0.23 ng/ml for pooled transformants. In contrast, untransformed cells secreted >10 ng/ml of the antigen. In addition to the reduction in *gag* RNA and p24 levels, HIV-1–infected, transformed cells contained significantly less (as much as 100 times) HIV-1 proviral DNA sequence compared to their infected, untransformed counterparts (*21*). This suggests, albeit indirectly, that constitutively expressed ribozymes can cleave incoming viral RNA genomes. A greater reduction in proviral DNA was seen in pooled compared to cloned cells (*21*), which correlated with the more pronounced reduction in *gag* RNA (Fig. 4b).

The potential deleterious effect of constitutively expressed catalyst on cell viability was evaluated in a short-term growth analysis. Transformed and untransformed (parental) cells were indistinguishable with respect to viability (>99% by trypan blue exclusion) and plating efficiency (>90%) at days 1, 2, 5, and 9 after seeding. The average doubling time over a 9-day period was 24.2 hours for parental cells and 23.1 hours for ribozyme-containing cells. Their RNA and DNA contents were the same and no morphological differences were detected (*21*). Cells expressing functional catalysts that have been in culture for more than 9 months show no signs of cytotoxicity.

Experiments presented here show stable expression of biologically active catalytic RNAs within a complex intracellular environment in the absence of cytotoxicity. Endogenous expression of an anti-*gag* catalytic RNA caused a diminution in viral-encoded *gag* RNA, proviral DNA, and p24 antigen. That a reduction in HIV *gag* RNA occurs concomitantly with a substantial reduction (20- to 40-fold) in p24 indicates that ribozymes can affect HIV-1 replication. Although it is conceivable that cleavage is mediated by a mechanism independent of catalytic RNAs, total RNA extracted from transfected cells retains the ability to cleave HIV *gag* RNA in a cell-free system (*16*), indicating that cleavage can be mediated by an RNA component alone.

As with any anti–HIV-1 therapeutic strategy, the problem of a high mutability rate that may abolish the site of cleavage must be addressed. Work with oligonucleotides as inhibitors of gene expression has shown that target sequences proximal to highly conserved regions (that is, AUG translation initiation codon, splice sites, single-strand loops in hairpin structures) are more accessible to binding (*22*). These sites and binding sites for viral regulatory factors (that is, *tat* and *rev*), whose functions are extremely sensitive to genetic variations are logical targets for catalytic RNAs. Alternatively, a multivalent ribozyme directed to multiple cleavage sites along a single RNA transcript may increase the probability that at least one of the target sites will be cleaved. By cleaving RNA targets at specific sites, catalytic RNAs offer a means for reducing the level of deleterious RNAs. Ribozymes thus represent a newly emerging class of potential anti–HIV-1 agents. Once combined with gene therapy, the full potential of ribozymes as therapeutic agents should be realized.

REFERENCES AND NOTES

1. J. G. Izant and H. Weintraub, *Cell* **36**, 1007 (1984); R. Harland and H. Weintraub, *J. Cell. Biol.* **101**, 109 (1985); D. Melton, *Proc. Natl. Acad. Sci. U.S.A.* **82**, 144 (1985).
2. T. R. Cech and B. Bass, *Annu. Rev. Biochem.* **55**, 599 (1986).
3. J. M. Buzayan *et al.*, *Nature* **323**, 349 (1986).
4. G. A. Prody *et al.*, *Science* **231**, 1577 (1986).
5. C. J. Hutchins *et al.*, *Nucleic Acids Res.* **14**, 3627 (1986).
6. P. Keese and R. H. Symons, in *Viroids and Viroid-Like Pathogens*, J. S. Semancik, Ed. (CRC Press, Boca Raton, FL, 1987), pp. 1–47.
7. R. Tritz and A. Hampel, *Biochemistry* **28**, 4929 (1989).
8. A. C. Forster and R. H. Symons, *Cell* **49**, 211 (1987).
9. R. H. Symons, *Trends Biochem.* **14**, 445 (1989).
10. L. Epstein and J. Gall, *Cell* **48**, 535 (1987).
11. O. C. Uhlenbeck, *Nature* **328**, 596 (1987).
12. C. C. Sheldon and R. H. Symons, *Nucleic Acids Res.* **17**, 5679 (1989).
13. M. Koizumi *et al.*, *ibid.*, p. 7059.
14. J. Haseloff and W. L. Gerlach, *Nature* **334**, 585 (1988).
15. L. Ratner *et al.*, *AIDS Res. Hum. Retroviruses* **3**, 57 (1987).
16. P. S. Chang *et al.*, *Clinical Biotech.* **2**, 1 (1990).
17. P. Gunning *et al.*, *Proc. Natl. Acad. Sci. U.S.A.* **84**, 4831 (1987).
18. P. J. Maddon *et al.*, *Cell* **47**, 333 (1986).
19. R. K. Saiki *et al.*, *Science* **230**, 1350 (1985).
20. J. A. Zaia *et al.*, *J. Virol.* **62**, 3914 (1988).
21. N. Sarver *et al.*, unpublished observations.
22. J. Goodchild *et al.*, *Proc. Natl. Acad. Sci. U.S.A.* **85**, 5507 (1988).
23. G. Murakawa *et al.*, *DNA* **7**, 287 (1988).

24. We thank J. Rosenberg for his constant support; J. Chen for expert technical assistance; and M. Johnston and J. McGowan for provocative discussions and critical reading of the manuscript. Supported by a PHS, National Institute of Allergy and Infectious Diseases National Cooperative Drug Discovery Grant (AI25959) to E.C., J.Z. and J.R.; E.C., J.Z., and J.R. are members of the City of Hope Cancer Center (CA34991); P.C. was supported in part by a Medical Scientists Training Program fellowship from Loma Linda University, School of Medicine.

11 October 1989; accepted 29 December 1989

A T Cell–Specific Transcriptional Enhancer Within the Human T Cell Receptor δ Locus

JUAN MIGUEL REDONDO, SHINGO HATA,* CATHY BROCKLEHURST, MICHAEL S. KRANGEL

The T cell antigen receptor (TCR) δ gene is located within the TCRα locus. A T cell–specific transcriptional enhancer, distinct from the TCRα enhancer, has been identified within the $J_\delta 3$-C_δ intron of the human T cell receptor δ gene. This enhancer activates transcription from the $V_\delta 1$ and $V_\delta 3$ promoters as well as from heterologous promoters. Enhancer activity has been localized to a 250-bp region that contains multiple binding sites for nuclear proteins. Thus, transcriptional control of the TCRδ and TCRα genes is mediated by distinct regulatory elements.

EXPRESSION OF THE REARRANGING genes that encode the immunoglobulin (Ig) and TCR polypeptides is controlled in part by promoter elements associated with the variable (V) gene segments and enhancer elements associated with the constant (C) gene segments (*1*). Such elements are separated by large distances in the germline configuration, but are brought into proximity by the rearrangement of V segments to diversity (D) and joining (J) segments, thereby inducing selective expression of the rearranged gene. Tissue-specific transcriptional enhancer ele-